Virologica Sinica (2021) 36:1165–1176
https://doi.org/10.1007/s12250-021-00404-9

www.virosin.org
www.springer.com/12250

RESEARCH ARTICLE

Cucurbit[7]uril as a Broad-Spectrum Antiviral Agent against Diverse RNA Viruses

Jia Quan[1] · Xiangjun Zhang[2] · Yuanfu Ding[2] · Shengke Li[2] · Yang Qiu[3] · Ruibing Wang[2] · Xi Zhou[1,3]

Received: 25 March 2021 / Accepted: 6 April 2021 / Published online: 26 May 2021

Abstract

The emergence and re-emergence of RNA virus outbreaks highlight the urgent need for the development of broad-spectrum antivirals. Polyamines are positively-charged small molecules required for the infectivity of a wide range of RNA viruses, therefore may become good antiviral targets. Cucurbit[7]uril (CB[7]), a synthetic macrocyclic molecule, which can bind with amine-based organic compounds with high affinity, has been shown to regulate bioactive molecules through competitive binding. In this study, we tested the antiviral activity of CB[7] against diverse RNA viruses, including a panel of enteroviruses (i.e. human enterovirus A71, coxsackievirus A16, coxsackievirus B3, and echovirus 11), some flaviviruses (i.e. dengue virus and Zika virus), and an alphavirus representative Semliki forest virus. CB[7] can inhibit virus replications in a variety of cell lines, and its mechanism of action is through the competitive binding with polyamines. Our findings not only for the first time provide evidence that CB[7] can be a promising broad-spectrum antiviral agent, but more importantly, offer a novel therapeutic strategy to fight against RNA viruses by supramolecular sequestration of polyamines.

Keywords Cucurbit[7] (CB[7]) · RNA viruses · Broad-spectrum antiviral activity

Introduction

The emergence and re-emergence of RNA virus outbreak highlight the urgent need for the development of broad-spectrum antivirals. Currently, broad-spectrum antivirals can be classified into several broad categories, including interferon and/or interferon inducers to stimulate host immune response, nucleotide analogs that resemble cellular DNA or RNA nucleotide and inhibit viral RNA replication, transcription or translation, and compounds or peptides that block entry of diverse viruses.

Polyamines, including putrescine, spermidine and spermine, are a class of positively charged small molecules derived from ornithine, and are ubiquitously and abundantly present in cells at concentrations up to 1.0 mmol/L (Igarashi and Kashiwagi 2000). Almost 80% of cellular polyamines directly bind to RNA (Igarashi and Kashiwagi 2015), and they have been found to participate in multiple cellular processes, including RNA folding, protein-RNA interactions, DNA structure formation, mRNA translation, and modulating membrane fluidity (Schipper *et al.* 2000; Gerner and Meyskens 2004; Mandal *et al.* 2013). Apart from various cellular processes, polyamines also play important roles in viral life cycles. It was reported that polyamines participate in the replication of a wide range of RNA viruses, such as enterovirus, flavivirus, alphavirus, vesiculovirus, bunyavirus, and filovirus (Mounce *et al.* 2016b; Kicmal *et al.* 2019; Mastrodomenico *et al.* 2019). Polyamines are also required for viral protein translation and keeping viral RNA-dependent RNA polymerase activity in the life cycle of viruses such as Chikungunya virus and Zika virus (ZIKV) (Mounce *et al.* 2016b, 2017).

✉ Xi Zhou
zhouxi@wh.iov.cn

✉ Ruibing Wang
rwang@um.edu.mo

[1] State Key Laboratory of Virology, College of Life Sciences, Wuhan University, Wuhan 430072, China

[2] State Key Laboratory of Quality Research in Chinese Medicine, Institute of Chinese Medical Sciences, University of Macau, Macau 999078, China

[3] State Key Laboratory of Virology, Wuhan Institute of Virology, Center for Biosafety Mega-Science, Chinese Academy of Sciences, Wuhan 430071, China

In addition, deletion of polyamine synthase suppressed the hypusination of eukaryotic initiation factor 5A that is required for both gene expression and viral replication of Ebola virus (Olsen *et al*. 2018). Moreover, polyamines were shown to be essential for maintaining the infectivity of Rift Valley fever virus and La Crosse virus, and polyamine depletion resulted in the accumulation of interfering noninfectious particles that limit infectivity (Mastrodomenico *et al*. 2019). Therefore, the biosynthetic process of polyamines has been considered as a potential ideal target for developing broad-spectrum antivirals against diverse RNA viruses, including many important human pathogens. For instance, difluoromethylornithine (DFMO), an FDA-approved specific inhibitor of ornithine decarboxylase (ODC1) that mediates the synthesis of polyamines from ornithine, has been found to inhibit the replication of various RNA viruses (Mounce *et al.* 2016b). However, targeting a pivotal host enzyme may result in an unexpected side effect, while direct sequestration of polyamine may provide a rapid and reversible, alternative approach in restricting the replication of multiple RNA viruses.

Cucurbit[*n*]uril (CB[*n*], *n* = 5–8, 10, 14), a group of pumpkin-shaped macrocyclic glycoluril oligomers linked via methylene groups, possess a hydrophobic cavity fringed with two hydrophilic carbonyl portals that preferably bind with amine-based organic compounds with high affinity (Assaf and Nau 2015; Barrow *et al.* 2015). Within this family, CB[7] has attracted increasing attention for biomedical applications, attributed to its decent water solubility, biocompatibility and appropriate cavity size that can accommodate a variety of bioactive guest molecules, including amine-containing molecules such as polyamines (Shetty *et al.* 2015; Kuok *et al.* 2017). In particular, CB[7] has been shown to regulate the physiological functions of bioactive molecules through competitively inhibiting their binding with non-target and target biological receptors (Kuok *et al.* 2017; Zhang *et al.* 2019b; Yin *et al.* 2021). For instance, supramolecular encapsulation of polyamines by CB[7] was used to control polyamine-induced conformational changes of DNA, due to the higher binding between polyamines with CB[7] than that with DNA (Parente Carvalho *et al.* 2015; Wang *et al.* 2018; Chernikova and Berdnikova 2020). In addition, *in vitro* and *in vivo* sequestration of paraquat by CB[7] was recently shown to successfully reverse and control the toxicity of the guest species (Zhang *et al*. 2019a). Therefore, we hypothesized that CB[7] could potentially exert antiviral effects against RNA viruses via supramolecular encapsulation of endogenous cellular polyamines.

In this work, the broad-spectrum antiviral effects of CB[7] against diverse RNA viruses, including human enterovirus A71 (EV-A71), coxsackievirus A16 (CVA16), coxsackievirus B3 (CVB3), echovirus 11 (Echo-11), Semliki forest virus (SFV), dengue virus 2 (DENV2) and ZIKV were uncovered for the first time. The relationship between the antiviral activity of CB[7] and the polyamine pathway was also investigated.

Materials and Methods

Cell Culture and CB[7]

Human rhabdomyosarcoma (RD) cells, human non-small cell lung cancer A549 cells, human colon adenocarcinoma Caco2 cells, human cervical carcinoma HeLa cells, human embryonic kidney HEK293T cells, green monkey kidney Vero cells and Baby Hamster Syrian Kidney BHK-21 cells were purchased from ATCC (American Type Culture Collection) and maintained in Dulbecco modified Eagle medium (DMEM; Gibco, China) supplemented with 10% fetal bovine serum (FBS; Gibco, Australia), 100 U/mL penicillin, and 100 g/mL streptomycin (HyClone; Austria) at 37 °C in an incubator with 5% CO_2. *Aedes aegypti* Aag2 cells (ATCC, CCL-125) were cultured at 27.5 °C in Schneider's insect medium (Gibco) supplemented with 10% fetal bovine serum (FBS; Gibco). *Aedes albopictus* C6/36 cells (ATCC CRL-1660) were cultured in RPMI 1640 (Thermo Fisher Scientific, China) medium containing 10% FBS at 27.5 °C. CB[7] ($C_{42}H_{42}N_{28}O_{14}$, molecular weight: 1162.96 g/mol) was synthesized as described previously (Kim *et al.* 2000; Bardelang *et al.* 2011).

Viruses

EV-A71 strain H VR-1432 were obtained from ATCC, and CV-A16 GD09/24 were kindly provided by Dr. Cheng-Feng Qin (Beijing, China), and CVB3 Wooddruff was kindly provided by Dr. Zhaohua Zhong (Harbin, China). The clinical strain of EV-A71 (XY833) was obtained from Hubei Province Center for Disease Control and Prevention (Hubei, China). The clinical strain of Echo-11 (GWCMC01/GZ/CHN/2019) was obtained from Guangzhou Women and Children's Medical Center (Guangzhou, China). These viruses were amplified and titers were determined in RD cells. ZIKV strain GZ01 and DENV2 strain TSV01 were kindly provided by Dr. Cheng-Feng Qin and amplified in C6/36 cells and titrated by plaque assay in BHK-21 cells, respectively. SFV was generated from an infectious cDNA clone of SFV4 kindly provided by Dr. Tero Ahola (Helsinki, Finland) and amplified in 293T cells and titrated by plaque assay in Vero cells.

Virus Infection and Plaque Assays

In mammalian cells, at the day of infection, the medium was changed with 2% FBS–DMEM, and then the viruses were added to cells at an MOI of 0.1. Total RNAs were extracted at 24 or 48 h post-infection (hpi) and subjected to qRT-PCR analysis. For plaque assays, Vero cells in 12-well plates were infected with supernatants from the infected-RD cells treated with CB[7]. The cells were cultured at 37 °C for 2 h to allow the adsorption of all the viruses. The supernatant was then replaced with MEM containing 2% FBS and 1% penicillin–streptomycin with isopycnic 1% low-melting-point agarose (Sigma-Aldrich, Japan). After incubation at 37 °C for 72 h, cells were fixed with 10% formaldehyde and stained with 0.5% crystal violet at 4 °C for 2 h.

Western Blotting

Cells were harvested in lysis buffer (50 mmol/L Tris–HCl [pH 7.4], 150 mmol/L NaCl, 1% NP-40, 0.25% deoxycholate, and a protease inhibitor cocktail [Roche]). The lysates were then subjected to 12% SDS-PAGE and Western blotting according to our standard procedures (Zhou *et al.* 2020). The antibodies used in this study are included anti-tubulin (Protein Tech Group, 1:3000), anti-VP1 (Abnova, 1:1000), anti-Zika virus Envelope protein (GeneTex GTX133314).

RNA Extraction and qRT-PCR

Viral or cellular RNAs were extracted using the Purelink RNA mini kit (Thermo Fisher Scientific) according to the manufacturer's instructions. Virus genomic RNA was quantified by one step PrimeScriptTM RT-qPCR Kit (Takara, Japan). IFN pathway-related gene transcripts were quantified using a one-step SYBR green RT-PCR Kit (Takara).

siRNA Transfection and CCK-8 Assay

ODC1 siRNA and SAT1 siRNA duplexes were purchased from RIBOBIO, China. Silencer Negative Control siRNA (siNC) was used as negative control and does not target any endogenous transcript. The siRNA transfection was performed according to the manufacture's instructions.

The cytotoxicity of CB[7] was detected by using a Cell Counting Kit (CCK-8, Beyotime, China) following the manufacturer's instruction. Briefly, 100 μL cells (1×10^5 mL^{-1}) were seeded into the wells of a 96-well microtiter plate and incubated at 37 °C for 12 h. Then CB[7] at graded concentrations was added. After incubation at 37 °C for 24 h, 10 μL of CCK-8 solution were added, followed by an additional incubation for 2 h. The absorbance was measured at 450 nm.

Quantification and Statistical Analysis

GraphPad Prism 8.0 was used for statistical analyses. All experiments were repeated at least three times. Statistical analysis was carried out by unpaired *t* test. P value < 0.05 was considered statistically significant.

Results

CB[7] Inhibits the Replication of Enteroviruses

The supramolecular chemistry between CB[7] and polyamines have been well-studied and multiple evidence have shown that CB[7] exhibits higher binding affinity with different polyamines, including putrescine, spermidine and spermine, than nucleic acids (Table 1). Therefore, we sought to examine whether the sequestration of polyamines by CB[7] could exert any antiviral activity. To this end, EV-A71 that belongs to the genus *Enterovirus* of the family *Picornaviridae* and is the major causative pathogen for hand-foot-and-mouth disease (HFMD) was used for the initial investigation. We used EV-A71 (strain H, VR-1432) that is a common strain for laboratory research. Rhabdomyosarcoma (RD) cells were pretreated with increasing concentrations of CB[7] for 2 h and then infected with EV-A71 for one hour at a multiplicity of infection (MOI) of 0.1. At 24 hpi, the antiviral effect of CB[7] was determined via measuring viral RNA accumulation with qRT-PCR. Our data showed that CB[7] exerted potent anti-EV-A71 activity in a dose-dependent manner, with the 50% inhibitory concentration (IC_{50}) value of 344 ± 24.24 μmol/L (Fig. 1A). Besides, the cytotoxicity of CB[7] in RD cells was examined via CCK-8, and the 50% cytotoxic concentration (CC_{50}) of CB[7] in RD cells is greater than 2500 μmol/L (Fig. 1B). Moreover, this anti-EV-A71 effect of CB[7] was also confirmed by measuring virus titers in infected cells via plaque assays (Fig. 1C, 1D) or determining EV-A71 coat protein VP1 via Western blotting (Fig. 1E), respectively. With the promising antiviral effects of CB[7] on the common strain of EV-A71 (strain H, VR-1432), we further tested the effect of CB[7] on a clinical strain of EV-A71 (strain XY833) in RD cells, and found that the IC_{50} value of CB[7] against this clinical isolated strain is 346.6 ± 17.98 μmol/L. (Fig. 1F).

We further examined the inhibitory effects of CB[7] on EV-A71 in different cell lines, including human cervical carcinoma HeLa cells, green monkey kidney Vero cells, and human colon adenocarcinoma CaCo-2 cells, via

Table 1 Binding affinities of polyamines and CB[7] or nucleic acids.

Polyamines	Nucleic acids/CB[7]	Methods	Binding constants (Ka, M^{-1})	References
Putrescine	CB[7]	Fluorescence titration in 10 mmol/L NH_4OAc buffer of pH 6.0 at ambient temperature	3.7×10^5	Hennig *et al.* (2007)
Spermidine	CB[7]	ITC titration in 100 μmol/L $CaCl_2$, NaCl and $NaHCO_3$ at 25 °C	2.2×10^5	Da Silva *et al.* (2014)
Spermine	CB[7]	ITC titration in 20 mmol/L PBS buffer of pH 6.0 at 37 °C	1.18×10^6	Chen *et al.* (2017)
Putrescine	DNA	Affinity capillary electrophoresis method in 20 mmol/L Tris–HCl buffer of pH 7.0 at 25 °C	1.02×10^5	Ouameur and Tajmir-Riahi (2004)
Spermidine	DNA	Affinity capillary electrophoresis method in 20 mmol/L Tris–HCl buffer of pH 7.0 at 25 °C	1.4×10^5	Ouameur and Tajmir-Riahi (2004)
Spermine	DNA	Affinity capillary electrophoresis method in 20 mmol/L Tris–HCl buffer of pH 7.0 at 25 °C	2.3×10^5	Ouameur and Tajmir-Riahi (2004)
Spermine	DNA	Gel filtration method in 100 mmol/L Tris–HCl, 2 mmol/L Mg^{2+} and 100 mmol/L K^+ buffer of pH 7.5 at 4 °C	$10^3 \sim 10^5$	Igarashi *et al.* (1982)
Spermidine	16S rRNA	Gel filtration method in 100 mmol/L Tris–HCl, 2 mmol/L Mg^{2+} and 100 mmol/L K^+ buffer of pH 7.5 at 4 °C	2.2×10^3	Igarashi *et al.* (1982)
Spermine	16S rRNA	Gel filtration method in 100 mmol/L Tris–HCl, 2 mmol/L Mg^{2+} and 100 mmol/L K^+ buffer of pH 7.5 at 4 °C	1.8×10^4	Igarashi *et al.* (1982)

measuring viral RNA accumulation. As shown in Fig. 1G–1I, CB[7] treatment at a concentration of 625 μmol/L for 2 h significantly inhibited EV-A71 replication in all these cell lines. Besides, the CC_{50} values of CB[7] in these cell lines were all higher than 2500 μmol/L (Fig. 1J–1L).

Next, we sought to examine the antiviral effects of CB[7] on other enteroviruses, including CV-A16, CVB3 and Echo 11 that are causative pathogens for HFMD, myocarditis and neonatal sepsis-like disease, respectively. We pretreated RD cells with CB[7] prior to infection with CV-A16, CVB3 or Echo 11, respectively, and viral RNA accumulation was determined via qRT-PCR. Our data showed that CB[7] treatment effectively inhibited the replication of CV-A16 (Fig. 2A) with the IC_{50} values of 433.3 ± 36.04 μmol/L and Echo 11 with the IC_{50} values of 276.1 ± 33.12 μmol/L (Fig. 2B), respectively. And CVB3 was also found to be sensitive to CB[7] (Fig. 2C). Together, our findings indicate that CB[7] exhibits a potent broad-spectrum antiviral activity against diverse enteroviruses.

CB[7] Inhibits the Replication of Flaviviruses

To explore whether other RNA viruses are also sensitive to CB[7], we examined the antiviral activity of CB[7] against ZIKV that belongs to mosquito-borne flavivirus and is an important human pathogen for neonatal microcephaly (Yuan *et al.* 2017; Hu *et al.* 2019; Qiu *et al.* 2020). Human non-small cell lung cancer A549 cells were pretreated with various concentrations of CB[7] for 2 h before infection with ZIKV for 1 h at an MOI of 0.1, and the viral RNA accumulation was measuring via qRT-PCR at 24 hpi. We identified that CB[7] inhibited ZIKV replication in a dose-dependent manner, with IC_{50} value of 285.6 ± 19.42 μmol/L in A549 cells (Fig. 3A). The CC_{50} value of CB[7] in A549 cells is more than 2500 μmol/L (Fig. 3B). Besides, this anti-ZIKV effect of CB[7] was also confirmed by determining ZIKV envelope protein via Western blotting (Fig. 3C) and plaque assays (Fig. 3D−3E). Consistently, CB[7] also showed anti-ZIKV effect in baby hamster kidney BHK-21 cells (Fig. 3F).

Mosquito-borne flaviviruses were transmitted through vector mosquito to host mammals (Qiu *et al.* 2020). Thus, we sought to examine whether CB[7] could also inhibit ZIKV in mosquito cell lines, including *A. aegypti* Aag2 cells and *A. albopictus* C6/36 cells. As shown in Fig. 4A, 4B, CB[7] treatment efficiently inhibited ZIKV replication in these two cell lines, with the IC_{50} values of 426.5 ± 98.6 μmol/L in Aag2 cells and 560.1 ± 80.7 μmol/L in C6/36 cells, respectively. Besides, the CC_{50} values of CB[7] in these two cell lines are both greater than 2500 μmol/L (Fig. 4C, 4D).

We further examined the antiviral activity of CB[7] against DENV2, another important mosquito-borne

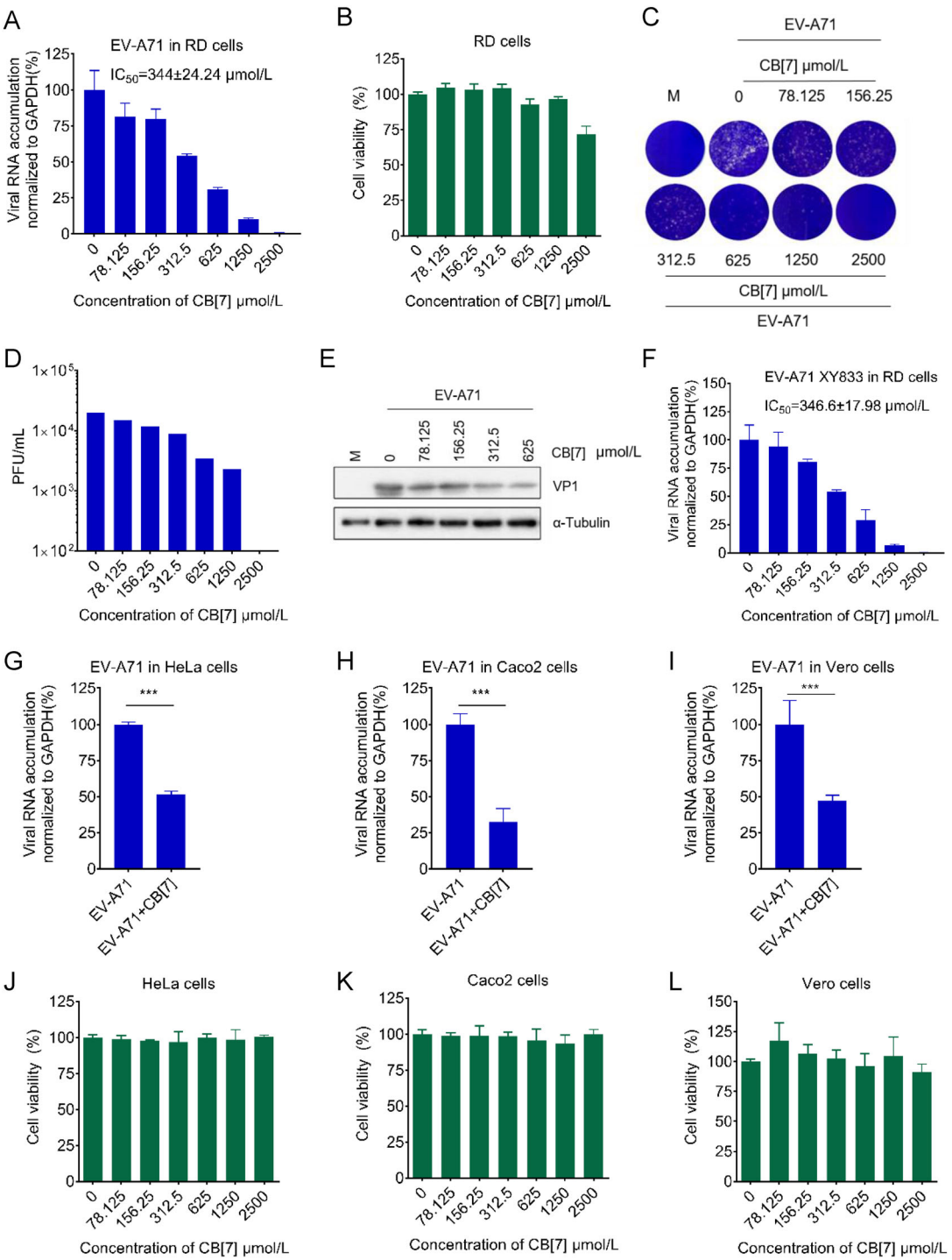

Fig. 1 CB[7] inhibits the replication of EV-A71. **A** RD cells were treated with CB[7] at various concentrations for 2 h, after that cells were washed by PBS and infected with EV-A71 at a MOI = 0.1 for 1 h, and then cells were washed by PBS for three times and CB[7] were added. Total RNAs were extracted at 24 hpi and viral RNA accumulation was measured via qRT-PCR. **B** Cell viability of RD cells determined with CCK-8 assay. **C** RD cells were pretreated with various concentrations of CB[7] before infection with EV-A71, and supernatant was collected at 24 hpi for plaque assay. **D** Quantification of viral titers. **E** Western blotting for EV-A71 VP1 protein in RD cells treated with CB[7]. **F** The antiviral effect of CB[7] against EV-A71 (XY-833) was determined as described in (**A**). **G–I** Antiviral effects of 625 μmol/L CB[7] for EV-A71 in HeLa cells, Caco-2 cells and Vero cells. **J–L** Cell viability of HeLa cells, Caco2 cells and Vero cells determined with CCK-8 assay. ***$P < 0.001$.

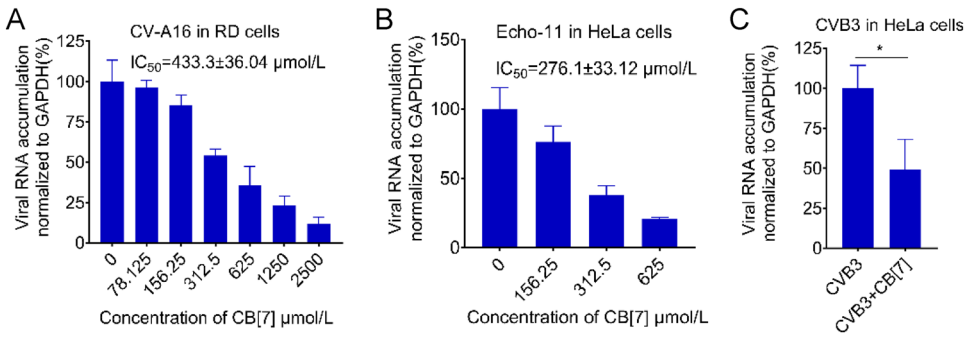

Fig. 2 CB[7] inhibits the replication of enteroviruses. **A–B** The antiviral effect of CB[7] against CV-A16 A in RD cells and Echo-11 **B** in HeLa cells were determined as described in Fig. 1A. **C** Antiviral effect of 625 μmol/L CB[7] for CVB3 in HeLa cells was measured via qRT-PCR. $*P < 0.05$.

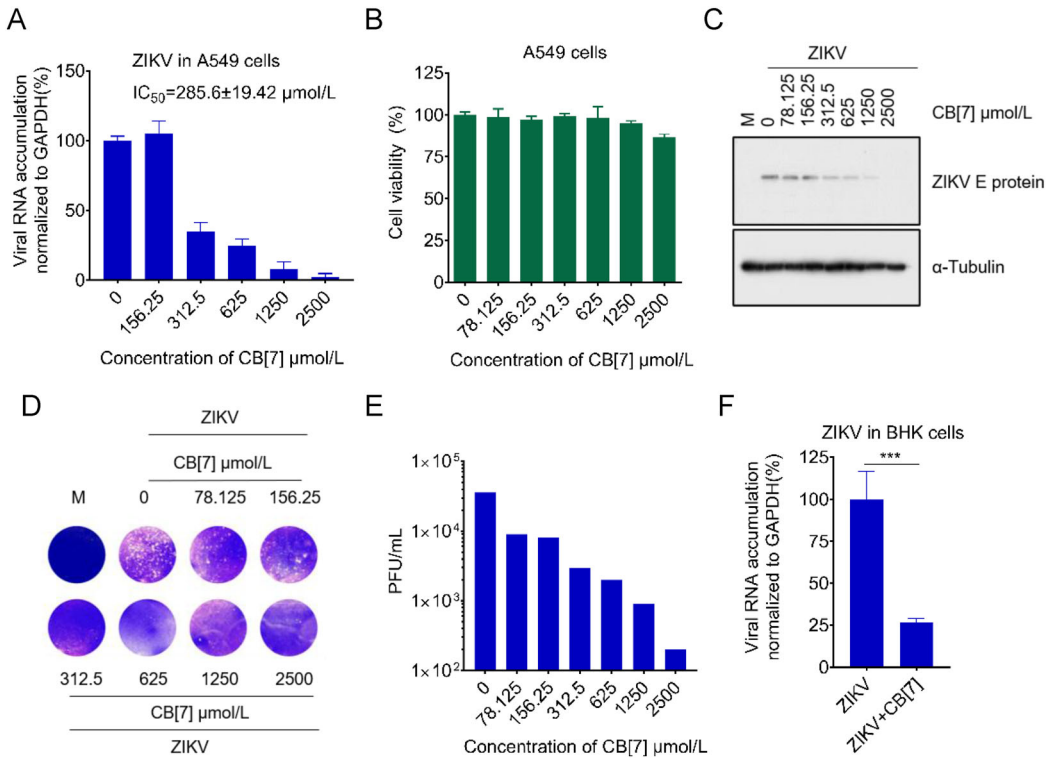

Fig. 3 CB[7] inhibits the replication of Zika virus. **A** A549 cells were treated with CB[7] at various concentrations for 2 h, after that cells were washed by PBS and infected with ZIKV at a MOI = 0.1 for 1 h, and then cells were washed by PBS for three times and CB[7] were added. Total RNAs were extracted at 24 hpi and viral RNA accumulation was measured via qRT-PCR. **B** CCK-8 assay for the cell viability of A549 cells determined with CCK-8 assay. **C** Western blotting for Zika virus Envelope protein in A549 cells treated with CB[7]. **D** A549 cells were pretreated with various concentrations of CB[7] before infection with ZIKV, and supernatant was collected at 24 hpi for plaque assay. **E** Quantification of viral titers. **F** Antiviral effect of 625 μmol/L CB[7] for ZIKV in BHK cells was measured via qRT-PCR. $***P < 0.001$.

flavivirus responsible for dengue hemorrhagic fever (Miao *et al.* 2019; Wang *et al.* 2020; Du *et al.* 2021), in Aag2 and C6/36 cells, respectively. As a result, the IC_{50} values of CB[7] anti-DENV2 are 420.2 ± 67.84 μmol/L in Aag2 and 379.3 ± 57.42 μmol/L in C6/36 cells, respectively (Fig. 4E, 4F). Together, our findings indicate that CB[7] can inhibit mosquito-borne flaviviruses in both mammalian and mosquito cells.

CB[7] Inhibits the Replication Alphavirus

We sought to expand our findings in other RNA viruses. Thus, we examined the effect of CB[7] on SFV, a prototypic alphavirus, in human embryonic kidney 293T cells. Consistent with the antiviral effects of CB[7] on enteroviruses and flaviviruses, CB[7] exerts anti-SFV activity in 293T cells in a dose-dependent manner, with IC_{50} value of 603.4 ± 64.65 μmol/L and CC_{50} value of more than 2500 μmol/L (Fig. 5A and 5B). Collectively, our data demonstrate that CB[7] possesses the broad-spectrum antiviral

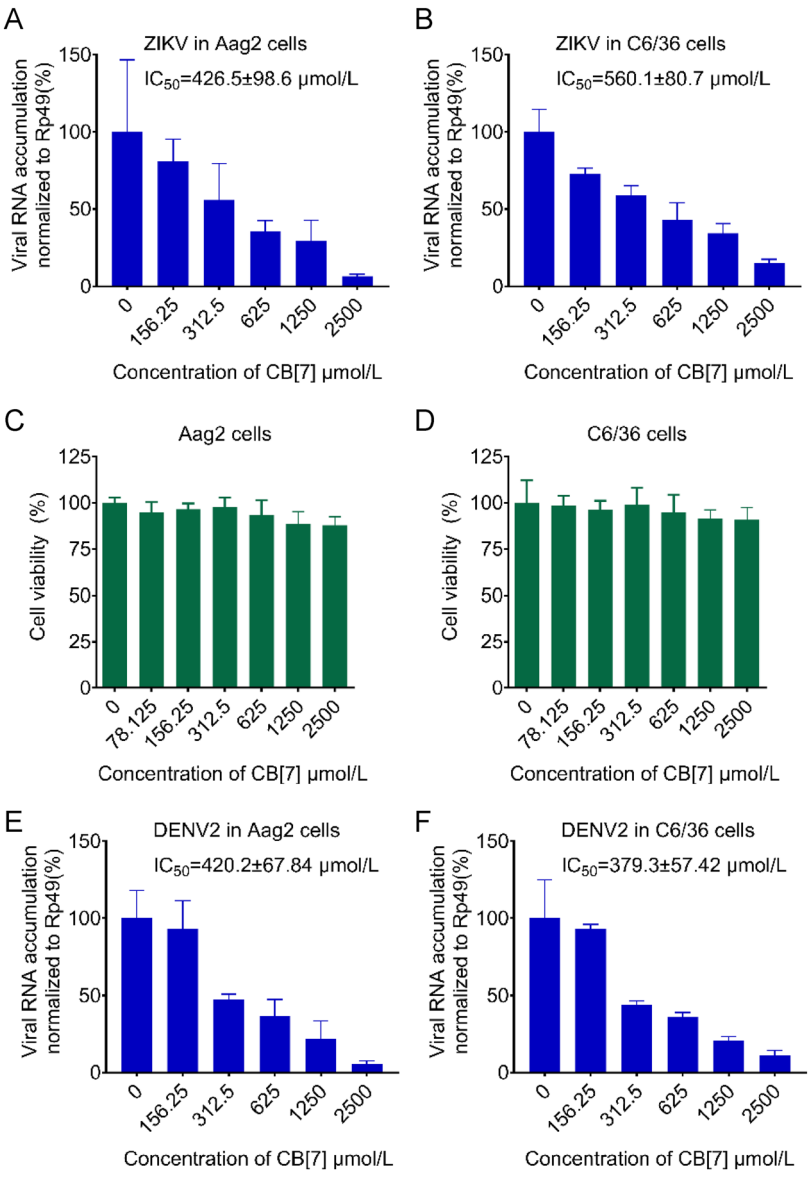

Fig. 4 CB[7] inhibits the replication of flaviviruses in mosquito cell lines. **A-B** Aag2 (**A**) and C6/36 (**B**) cells were treated with CB[7] at various concentrations for 2 h, after that cells were washed by PBS and infected with ZIKV at a MOI = 0.1 for 1 h, and then cells were washed by PBS for three times and CB[7] were added. Total RNAs were extracted at 24 hpi and viral RNA accumulation was measured via qRT-PCR. **C-D** Cell viability of Aag2 cells and C6/36 cells determined with CCK-8 assay. Aag2 **E** and C6/36 **F** cells were treated with CB[7] at various concentrations for 2 h, after that cells were washed by PBS and infected with DENV2 at a MOI = 0.1 for 1 h, and then cells were washed by PBS for three times and CB[7] were added. Total RNAs were extracted at 24 hpi and viral RNA accumulation was measured via qRT-PCR.

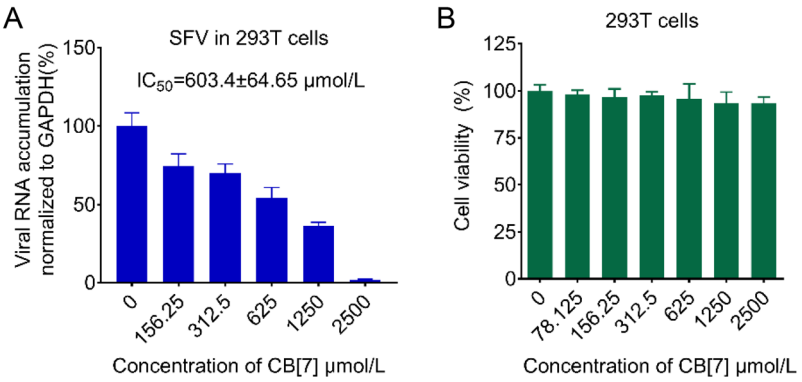

Fig. 5 CB[7] inhibits the replication of alphavirus. **A** 293 T cells were treated with CB[7] at various concentrations for 2 h, after that cells were washed by PBS and infected with SFV at a MOI = 0.1 for 1 h, and then cells were washed by PBS for three times and CB[7] were added. Total RNAs were extracted at 24 hpi and viral RNA accumulation was measured via qRT-PCR. **B** Cell viability of 293 T cells determined with CCK-8 assay.

effects against a wide range of RNA viruses in different cell lines.

Inhibition of the Polyamine Pathway Restricts the Antiviral Activity of CB[7]

After identifying that CB[7] can inhibit viral RNA replication of diverse RNA viruses, we sought to examine whether the broad-spectrum antiviral activity of CB[7] is directly related to polyamine depletion. To this end, we adopted an RNAi-based loss-of-function to target ODC1, which mediates polyamines production (Pegg 2008; Mounce *et al.* 2016b). Interestingly, in the presence of ODC1 knockdown (siODC1; Fig. 6A), the treatment of CB[7] failed to further inhibit the viral RNA accumulation of EV-A71 in RD cells (Fig. 6B), indicating that the anti-EV-A71 effect of CB[7] was absent in ODC1-deficient cells. Similarly, our data also showed that knockdown of ODC1 in A549 cells (Fig. 6C) impaired the antiviral activities of CB[7] against DENV2 and ZIKV (Fig. 6D–6E). Therefore, the antiviral activity of CB[7] is dependent on the polyamine pathway.

CB[7] Inhibits the Replication of RNA Virus through Sequestrating Polyamine

Moreover, we tested the effects of CB[7] on diverse RNA viruses in the presence of DFMO, an FDA-approved specific enzymatic inhibitor of ODC1. As shown in Fig. 7A–7D, DFMO treatment significantly inhibited the viral RNA replication of DENV2, ZIKV, CVB3 and Echo 11 in A549 and HeLa cells, respectively, in line with the previous observations (Mounce *et al.* 2016b; Kicmal *et al.* 2019). Moreover, our data showed that the antiviral effects of CB[7] against these viruses were remarkably inhibited in cells pre-treated with DFMO (Fig. 7E–7H).

To further confirm that the antiviral activity of CB[7] relies on polyamine, we sought to test the possibility that supplying additional polyamine could restore viral replication inhibited by CB[7]. Our data showed that supplementation of spermine restored the restricted replication of ZIKV and EV-A71 in A549 and RD cells treated with CB[7], respectively (Fig. 7I–7J). In addition, CB[7] treatment showed no effect on the gene expression levels of IFN-β as well as ISGs (Fig. 7K–7M), indicating that the

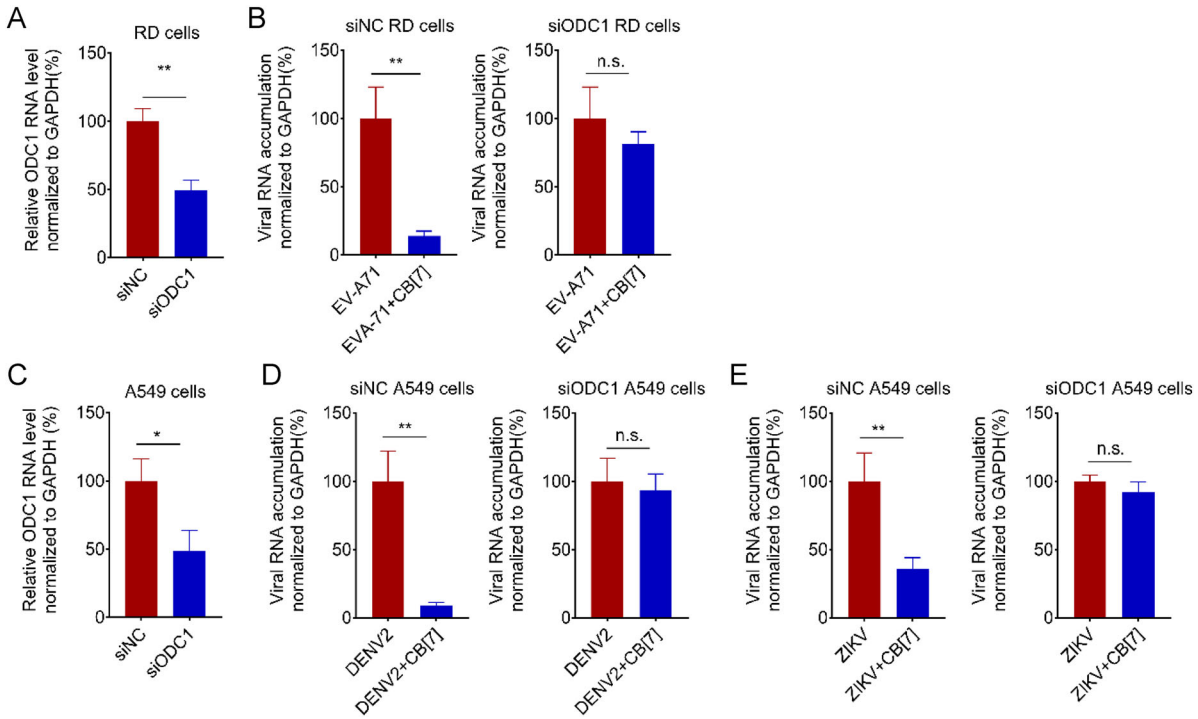

Fig. 6 The antiviral activity of CB[7] relies on the polyamine pathway. **A** ODC1 mRNA level in RD cells after transfected with 50 μmol/L of siODC1 for 24 h. **B** 50 μmol/L siRNAs targeting cellular ODC1 (siODC1) and 50 μmol/L negative control siRNAs (siNC) were transfected into RD cells, respectively, for 24 h. After that, the siRNA-transfected cells were pretreated with 1250 μmol/L CB[7] for 2 h and following infection with EV-A71 at an MOI of 0.1. **C** ODC1 mRNA level in A549 cells after transfected with 50 μmol/L of siODC1 for 24 h. **D–E** 50 μmol/L siRNAs targeting cellular ODC1 (siODC1) and 50 μmol/L negative control siRNAs (siNC) were transfected into A549 cells, respectively, for 24 h. After that, the siRNA-transfected cells were pretreated with 1250 μmol/L CB[7] for 2 h and following infection with DENV2 (**D**) or ZIKV(**E**) at an MOI of 0.1, respectively. Total RNAs were extracted at 24 hpi and viral RNA accumulation was measured via qRT-PCR with *t*-test (GraphPad Prism). $*P < 0.05$; $**P < 0.01$; n.s., no significance.

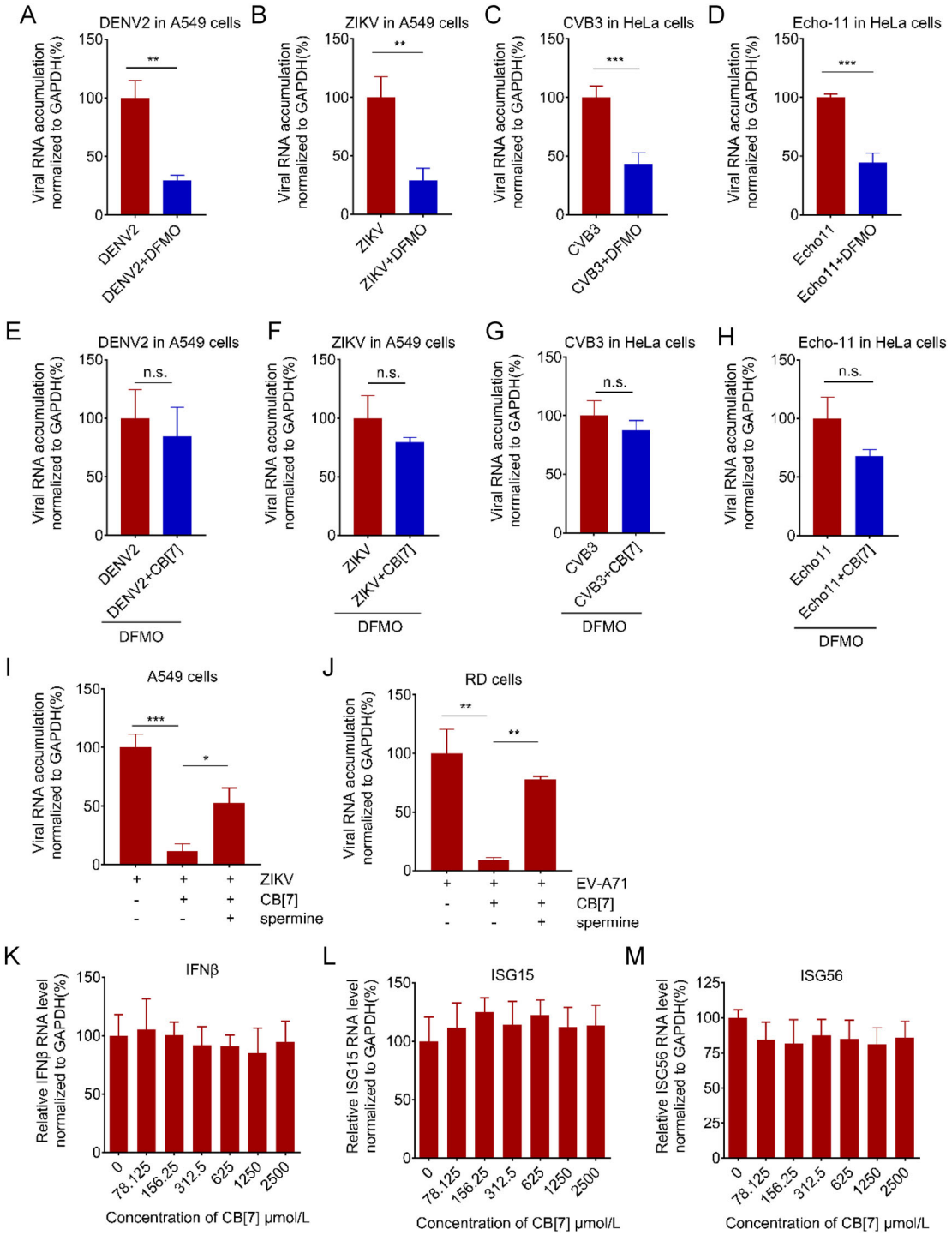

Fig. 7 Supplying additional polyamine impairs the antiviral activity of CB[7] and CB[7] shows no effect on the IFN system **A–D** 500 μmol/L DFMO were added to the indicated cells for 72 h, after that cells were infected with DENV2 (**A**), ZIKV (**B**), CVB3 (**C**) and Echo 11 (**D**) for 1 h, respectively. Cells were then washed with PBS and DFMO were added back to cells for additional 24 h. Total RNAs were extracted at 24 hpi and subjected to qRT-PCR. **E–H** The indicated cells were pretreated with 500 μmol/L DFMO for 72 h and then treated with 625 μmol/L CB[7] for 2 h, following infection with DENV2 (**E**), ZIKV (**F**), CVB3 (**G**) and Echo 11 (**H**). Total RNAs were extracted at 24 hpi and viral RNA accumulation was measured via qRT-PCR with *t*-test (GraphPad Prism). **I–J** A549 (**I**), RD (**J**) were treated with 1250 μmol/L CB[7] or 1250 μmol/L CB[7] plus 500 μmol/L spermine for 2 h before cells were infected with ZIKV or EV-A71. Total RNAs were extracted at 24 hpi and viral RNA accumulation was measured via qRT-PCR with *t*-test (GraphPad Prism). **K–M** A549 cells were treated with different concentrations of CB[7] for 24 h, total RNAs were extracted to test the mRNA level of indicated genes. $^{**}P < 0.01$; $^{***}P < 0.001$; n.s., no significance.

antiviral activity of CB[7] is not due to innate immune induction.

In summary, our findings demonstrate that CB[7] has a broad-spectrum antiviral activity against diverse RNA viruses through sequestrating polyamines.

Discussion

The increase in emergence and re-emergence of RNA virus outbreaks has underlined the urgent need to develop effective broad-spectrum antivirals for diverse RNA viruses (Metsky *et al.* 2017; Henry and Vikse 2020; Tuite *et al.* 2020). In this study, we provide the first demonstration that CB[7], a novel macrocyclic molecule, exhibits a potent broad-spectrum antiviral activity against a wide range of RNA viruses, including many important human pathogens. Mechanistically, we identified that the antiviral effect of CB[7] is dependent on polyamines.

CB[*n*] is a novel molecular container that could form stable complexes with various molecules, including drugs, amino acids, polyamines, peptides, and even high-molecular-weight molecules like proteins (Assaf and Nau 2015). Moreover, the strong host–guest binding between CB[n] and spermine was well demonstrated in supramolecular chemotherapy to realize the controlled release of the included drugs towards spermine overexpressed cancer cells (Chen *et al.* 2017). We noticed that the binding constant of polyamine with RNA is much low than that with CB[7] (Chernikova and Berdnikova 2020). Taking advantage of this feature, CB[7] has the potential to be a promising broad-spectrum antiviral drug that can restrict the replication of multiple RNA viruses through complexing and sequestering polyamines.

Previously, we have successfully demonstrated that CB[7] could inhibit/reverse the toxic effects of a series of exogenous bioactive molecules, including neurotoxins (Li *et al.* 2015; Zhang *et al.* 2019a), pesticides (Huang *et al.* 2018), anesthetics (Zhang *et al.* 2019b) and so on (Yin *et al.* 2021). Of note, oral administration of paraquat (PQ), a highly toxic pesticide, together with CB[7] in a mouse model significantly decreased PQ levels in the plasma and major organs and alleviated major organs' injuries (Zhang *et al.* 2019b). Moreover, oral administration of CB[7] within 2 h post-ingestion of PQ also significantly increased the survival rates and extended the survival time (Zhang *et al.* 2019b), suggesting that CB[7] can be applied orally as an antidote. In addition, we demonstrated that CB[7] injected orally, peritoneally and intravenously administered with the dose as high as 5 g/kg, 150 mg/kg and 500 mg/kg, respectively (Zhang *et al.* 2018). These previous studies indicate that CB[7] exhibits excellent safety profiles in mice, which provide important foundations for further investigations and clinical applications of CB[7]. Our future work will test the potential of CB[7] as antivirals *in vivo*.

The polyamine pathway plays pleiotropic roles at the different stages during viral infections for a wide range of RNA viruses. Accumulating evidence indicates that polyamines' biosynthetic process can be ideal targets for developing broad-spectrum antivirals against diverse RNA viruses, including many important human pathogens. Previous studies showed that DFMO treatment can efficiently suppress a wide range of RNA viruses by inhibiting polyamine synthesis enzyme ODC1 (Mounce *et al.* 2016a, 2016b). Herein, we provide an alternative approach to inhibit the infections of various RNA viruses by directly encapsulating polyamines with a synthetic receptor, CB[7], instead of inhibiting various polyamine synthase such as ODC1 that may influence other cellular functions (Gibson and Roizman 1971; Schipper *et al.* 2000; Gerner and Meyskens 2004; Choi *et al.* 2016; Jiang *et al.* 2018; Routhu *et al.* 2018; Sandusky-Beltran *et al.* 2019). Besides, considering that the physical and chemical properties of the guest drugs are often improved as a result of complexation, CB[7] combined with antiviral drugs with different antiviral mechanisms may have synergistic antiviral effects.

In summary, this work demonstrates that macrocyclic CB[7] exhibits a broad-spectrum antiviral effect against a wide range of RNA viruses by sequestrating polyamines. Our findings not only broaden the potential biomedical application of CB[7], but also provide a novel broad-spectrum antiviral drug. Via this action mechanism, other more specific artificial receptors of polyamines could be designed and synthesized as a new class of broad-spectrum antiviral drugs.

Acknowledgements We thank Dr. Cheng-Feng Qin (Beijing, China), Dr. Zhaohua Zhong (Harbin, China), Dr. Kun Cai (Hubei, China), Dr. Yi Xu (Guangzhou, China), Dr. Tero Ahola (Helsinki, Finland) and Dr. Martub L. Moore (Georgi, USA) for kindly providing materials. This work was supported by the Strategic Priority Research Program of CAS (XDB29010300 to X.Z.), International Partnership Program of Chinese Academy of Sciences (153B42KYSB20200004 to X.Z. and R.W.), National Natural Science Foundation of China (21871301 to R.W., 81873964 to Y.Q. and 31970169 to X.Z.), Grant from the CAS Youth Innovation Promotion Association (2020332 to Y.Q.). We are also grateful to the Science and Technology Development Fund, Macau SAR (0007/2020/A to R.W.) and the Science and Technology Bureau of Wuhan (2018060401011309 to X.Z.) for providing partial support to this work.

Author contributions JQ performed the experiments with the help of XJZ, YD and SL. YQ, RW and XZ designed the experiments, interpreted the results and wrote the manuscript.

Compliance with Ethical Standards

Conflict of interest The authors declare that they have no conflict of interest.

Animal and Human Rights Statement This article does not contain any studies with human or animal subjects performed by any of the authors.

References

Assaf KI, Nau WM (2015) Cucurbiturils: from synthesis to high-affinity binding and catalysis. Chem Soc Rev 44:394–418

Bardelang D, Udachin KA, Leek DM, Margeson JC, Chan G, Ratcliffe CI, Ripmeester JA (2011) Cucurbit[n]urils (n = 5–8): a comprehensive solid state study. Cryst Growth Des 11:5598–5614

Barrow SJ, Kasera S, Rowland MJ, del Barrio J, Scherman OA (2015) Cucurbituril-based molecular recognition. Chem Rev 115:12320–12406

Chen Y, Huang Z, Zhao H, Xu JF, Sun Z, Zhang X (2017) Supramolecular chemotherapy: cooperative enhancement of antitumor activity by combining controlled release of oxaliplatin and consuming of Spermine by Cucurbit[7]uril. ACS Appl Mater Interfaces 9:8602–8608

Chernikova EY, Berdnikova DV (2020) Cucurbiturils in nucleic acids research. Chem Commun 56:15360–15376

Choi Y, Oh ST, Won MA, Choi KM, Ko MJ, Seo D, Jeon TW, Baik IH, Ye SK, Park KU, Park IC, Jang BC, Seo JY, Lee YH (2016) Targeting ODC1 inhibits tumor growth through reduction of lipid metabolism in human hepatocellular carcinoma. Biochem Biophys Res Commun 478:1674–1681

Da Silva JP, Choudhury R, Porel M, Pischel U, Jockusch S, Hubbard PC, Ramamurthy V, Canário AV (2014) Synthetic versus natural receptors: supramolecular control of chemical sensing in fish. ACS Chem Biol 9:1432–1436

Du J, Zhang L, Hu X, Peng R, Wang G, Huang Y, Wang W, Wu K, Wang Q, Su H, Yang F, Zhang Y, Tang C, Cui X, Niu L, Lu G, Xiao M, Du Y, Yin F (2021) Phylogenetic analysis of the dengue virus strains causing the 2019 dengue fever outbreak in Hainan, China. Virol Sin. https://doi.org/10.1007/s12250-020-00335-x

Gerner EW, Meyskens FL Jr (2004) Polyamines and cancer: old molecules, new understanding. Nat Rev Cancer 4:781–792

Gibson W, Roizman B (1971) Compartmentalization of spermine and spermidine in the herpes simplex virion. Proc Natl Acad Sci U S A 68:2818–2821

Hennig A, Bakirci H, Nau WM (2007) Label-free continuous enzyme assays with macrocycle-fluorescent dye complexes. Nat Methods 4:629–632

Henry BM, Vikse J (2020) Clinical characteristics of Covid-19 in China. N Engl J Med 382:1860–1861

Hu T, Li J, Carr MJ, Duchêne S, Shi W (2019) The Asian lineage of Zika virus: transmission and evolution in Asia and the Americas. Virol Sin 34:1–8

Huang Q, Kuok KI, Zhang X, Yue L, Lee SMY, Zhang J, Wang R (2018) Inhibition of drug-induced seizure development in both zebrafish and mouse models by a synthetic nanoreceptor. Nanoscale 10:10333–10336

Igarashi K, Kashiwagi K (2000) Polyamines: mysterious modulators of cellular functions. Biochem Biophys Res Commun 271:559–564

Igarashi K, Kashiwagi K (2015) Modulation of protein synthesis by polyamines. IUBMB Life 67:160–169

Igarashi K, Sakamoto I, Goto N, Kashiwagi K, Honma R, Hirose S (1982) Interaction between polyamines and nucleic acids or phospholipids. Arch Biochem Biophys 219:438–443

Jiang F, Gao Y, Dong C, Xiong S (2018) ODC1 inhibits the inflammatory response and ROS-induced apoptosis in macrophages. Biochem Biophys Res Commun 504:734–741

Kicmal TM, Tate PM, Dial CN, Esin JJ, Mounce BC (2019) Polyamine depletion abrogates enterovirus cellular attachment. J Virol 93:e01054-19

Kim J, Jung I-S, Kim S-Y, Lee E, Kang J-K, Sakamoto S, Yamaguchi K, Kim K (2000) New Cucurbituril homologues: syntheses, isolation, characterization, and X-ray crystal structures of Cucurbit[n]uril (n = 5, 7, and 8). J Am Chem Soc 122:540–541

Kuok KI, Li S, Wyman IW, Wang R (2017) Cucurbit[7]uril: an emerging candidate for pharmaceutical excipients. Ann N Y Acad Sci 1398:108–119

Li S, Chen H, Yang X, Bardelang D, Wyman IW, Wan J, Lee SMY, Wang R (2015) Supramolecular Inhibition of Neurodegeneration by a Synthetic Receptor. ACS Med Chem Lett 6:1174–1178

Mandal S, Mandal A, Johansson HE, Orjalo AV, Park MH (2013) Depletion of cellular polyamines, spermidine and spermine, causes a total arrest in translation and growth in mammalian cells. Proc Natl Acad Sci U S A 110:2169–2174

Mastrodomenico V, Esin JJ, Graham ML, Tate PM, Hawkins GM, Sandler ZJ, Rademacher DJ, Kicmal TM, Dial CN, Mounce BC (2019) Polyamine depletion inhibits bunyavirus infection via generation of noninfectious interfering virions. J Virol 93:e00530-19

Metsky HC, Matranga CB, Wohl S, Schaffner SF, Freije CA, Winnicki SM, West K, Qu J, Baniecki ML, Gladden-Young A, Lin AE, Tomkins-Tinch CH, Ye SH, Park DJ, Luo CY, Barnes KG, Shah RR, Chak B, Barbosa-Lima G, Delatorre E, Vieira YR, Paul LM, Tan AL, Barcellona CM, Porcelli MC, Vasquez C, Cannons AC, Cone MR, Hogan KN, Kopp EW, Anzinger JJ, Garcia KF, Parham LA, Ramírez RMG, Montoya MCM, Rojas DP, Brown CM, Hennigan S, Sabina B, Scotland S, Gangavarapu K, Grubaugh ND, Oliveira G, Robles-Sikisaka R, Rambaut A, Gehrke L, Smole S, Halloran ME, Villar L, Mattar S, Lorenzana I, Cerbino-Neto J, Valim C, Degrave W, Bozza PT, Gnirke A, Andersen KG, Isern S, Michael SF, Bozza FA, Souza TML, Bosch I, Yozwiak NL, MacInnis BL, Sabeti PC (2017) Zika virus evolution and spread in the Americas. Nature 546:411–415

Miao M, Yu F, Wang D, Tong Y, Yang L, Xu J, Qiu Y, Zhou X, Zhao X (2019) Proteomics profiling of host cell response via protein expression and phosphorylation upon dengue virus infection. Virol Sin 34:549–562

Mounce BC, Cesaro T, Moratorio G, Hooikaas PJ, Yakovleva A, Werneke SW, Smith EC, Poirier EZ, Simon-Loriere E, Prot M, Tamietti C, Vitry S, Volle R, Khou C, Frenkiel MP, Sakuntabhai A, Delpeyroux F, Pardigon N, Flamand M, Barba-Spaeth G, Lafon M, Denison MR, Albert ML, Vignuzzi M (2016a) Inhibition of polyamine biosynthesis is a broad-spectrum strategy against RNA Viruses. J Virol 90:9683–9692

Mounce BC, Poirier EZ, Passoni G, Simon-Loriere E, Cesaro T, Prot M, Stapleford KA, Moratorio G, Sakuntabhai A, Levraud JP, Vignuzzi M (2016b) Interferon-Induced Spermidine-Spermine Acetyltransferase and Polyamine Depletion Restrict Zika and Chikungunya Viruses. Cell Host Microbe 20:167–177

Mounce BC, Cesaro T, Vlajnić L, Vidiņa A, Vallet T, Weger-Lucarelli J, Passoni G, Stapleford KA, Levraud JP, Vignuzzi M (2017) Chikungunya virus overcomes polyamine depletion by mutation of nsP1 and the opal stop codon to confer enhanced replication and fitness. J Virol 91:e00344-17

Olsen ME, Cressey TN, Mühlberger E, Connor JH (2018) Differential mechanisms for the involvement of polyamines and hypusinated eIF5A in ebola virus gene expression. J Virol 92:e01260-18

Ouameur AA, Tajmir-Riahi HA (2004) Structural analysis of DNA interactions with biogenic polyamines and cobalt(III)hexamine studied by Fourier transform infrared and capillary electrophoresis. J Biol Chem 279:42041–42054

Parente Carvalho C, Norouzy A, Ribeiro V, Nau WM, Pischel U (2015) Cucurbiturils as supramolecular inhibitors of DNA restriction by type II endonucleases. Org Biomol Chem 13:2866–2869

Pegg AE (2008) Spermidine/spermine-N1-acetyltransferase: a key metabolic regulator. Am J Physiol-Endocrinol Metab 294:E995–E1010

Qiu Y, Xu YP, Wang M, Miao M, Zhou H, Xu J, Kong J, Zheng D, Li RT, Zhang RR, Guo Y, Li XF, Cui J, Qin CF, Zhou X (2020) Flavivirus induces and antagonizes antiviral RNA interference in both mammals and mosquitoes. Sci Adv 6:eaax7989

Routhu NK, Xie Y, Dunworth M, Casero RA Jr, Oupicky D, Byrareddy SN (2018) Polymeric prodrugs targeting polyamine metabolism inhibit Zika Virus Replication. Mol Pharm 15:4284–4295

Sandusky-Beltran LA, Kovalenko A, Ma C, Calahatian JIT, Placides DS, Watler MD, Hunt JB, Darling AL, Baker JD, Blair LJ, Martin MD, Fontaine SN, Dickey CA, Lussier AL, Weeber EJ, Selenica MB, Nash KR, Gordon MN, Morgan D, Lee DC (2019) Spermidine/spermine-N(1)-acetyltransferase ablation impacts tauopathy-induced polyamine stress response. Alzheimers Res Ther 11:58

Schipper RG, Penning LC, Verhofstad AA (2000) Involvement of polyamines in apoptosis. Facts and controversies: effectors or protectors? Semin Cancer Biol 10:55–68

Shetty D, Khedkar JK, Park KM, Kim K (2015) Can we beat the biotin–avidin pair?: cucurbit[7]uril-based ultrahigh affinity host–guest complexes and their applications. Chem Soc Rev 44:8747–8761

Tuite AR, Ng V, Rees E, Fisman D (2020) Estimation of COVID-19 outbreak size in Italy. Lancet Infect Dis 20:537

Wang SR, Wang JQ, Xu GH, Wei L, Fu BS, Wu LY, Song YY, Yang XR, Li C, Liu SM, Zhou X (2018) The cucurbit[7]Uril-based supramolecular chemistry for reversible B/Z-DNA transition. Adv Sci 5:1800231

Wang R, Fan D, Wang L, Li Y, Zhou H, Gao N, An J (2020) Seroprevalence of dengue virus among young adults in Beijing, China, 2019. Virol Sin. https://doi.org/10.1007/s12250-020-00285-4

Yin H, Zhang X, Wei J, Lu S, Bardelang D, Wang R (2021) Recent advances in supramolecular antidotes. Theranostics 11:1513–1526

Yuan L, Huang XY, Liu ZY, Zhang F, Zhu XL, Yu JY, Ji X, Xu YP, Li G, Li C, Wang HJ, Deng YQ, Wu M, Cheng ML, Ye Q, Xie DY, Li XF, Wang X, Shi W, Hu B, Shi PY, Xu Z, Qin CF (2017) A single mutation in the prM protein of Zika virus contributes to fetal microcephaly. Science 358:933–936

Zhang X, Xu X, Li S, Wang LH, Zhang J, Wang R (2018) A systematic evaluation of the biocompatibility of cucurbit[7]uril in mice. Sci Rep 8:8819

Zhang X, Cheng Q, Li L, Shangguan L, Li C, Li S, Huang F, Zhang J, Wang R (2019a) Supramolecular therapeutics to treat the side effects induced by a depolarizing neuromuscular blocking agent. Theranostics 9:3107–3121

Zhang X, Xu X, Li S, Li L, Zhang J, Wang R (2019b) A synthetic receptor as a specific antidote for paraquat poisoning. Theranostics 9:633–645

Zhou H, Qian Q, Shu T, Xu J, Kong J, Mu J, Qiu Y, Zhou X (2020) Hepatitis C Virus NS2 protein suppresses RNA interference in cells. Virol Sin 35:436–444